MACROKINETICS OF AN AUTOWAVE MODE OF SYNTHESIS OF ORGANIC POWDERS IN A CONDENSED PHASE. 2. STRUCTURAL TRANSFORMATIONS IN A WAVE OF SELF-PROPAGATING SYNTHESIS OF ORGANIC POWDERS

A. D. Ubortsev, B. M. Khusid, Z. P. Zhul'man, A. G. Merzhanov, and V. A. Mansurov

UDC 536.46.5.24:541.128

Structural transformations in the front of an autowave mode of synthesis of organic powders in a condensed phase are studied. A mode of the front stopping and an initial acceleration section are considered. The dynamics of structural transformations and the effect of the heat exchange rate on the autowave mode are established.

Introduction. We have considered structural and physicochemical transformations in a wave of self-propagating synthesis, proceeding in mixtures of organic powders. The first part of the study has analyzed various autowave processes. The difference has been shown between self-propagating synthesis and the combustion of pyrotechnic compositions on the basis of organic matters. It has been discovered that the autowave modes in the mixture of organic powders involve a variation in electrochemical properties. The processes occurring in the wave and during synthesis in a calorimeter have been described. A qualitative difference in the given modes has been indicated. An understanding of the physicochemical conditions, elucidation of the internal mechanisms, and the substantiation of theoretical inferences necessitate a qualitative investigation and a visualization of autowave modes [1].

Methods of Optical Studies. 1. Autowavemode. Figure 1a shows a block diagram of the experimental setup. A vessel with the sample was placed in a constant-temperature shell of quartz glass. The temperature mode, assigned therein, was maintained using a thermostat. Light sources were a DRSh-150 mercury lamp with filter SS-8, and an incandescent lamp of power 100 W with filters KS-11 and ZS-1. Each of the sources is provided with a focusing system. The processes were visualized with the aid of a camera equipped with an auxiliary optical system, and with the filters ZhS-19 and OS-6. This bench permits, alongside of filming, monitoring of the image transmission. In the experiments, we used a cell for supervising the process of interaction between two individual crystals (Fig. 1b) and a plane cell for studying the front structure (Fig. 1c), as well as an MBI-7 microscope. Copper–constant thermocouples were installed into the cells for controlling temperature.

The original substances and the reaction product are colorless crystals [2]. For visualizing and identifying possible regions of the synthesis front we utilized dyes, viz., the chemical tracer methyl orange and fluorescein both in acid and base forms. The acid fluorescein was added to malonic acid, whereas the base one was added to piperazine. Crushed samples of malonic acid and fluorescein (2% by mass in relation to the acid) were dissolved in absolute ether. The dye solution was added by drops to the acid solution with a vigorous agitation. The mixture produced was settled until a precipitate was obtained, which was separated by decantation. The remaining ether was evaporated, and the yellow crystals formed of malonic acid were dried in vacuum and thereon in a desiccator above silica gel. Piperazine was dyed similarly, and reddish crystals were produced. Afterwards, a stoichiometric mixture was prepared from one dyed and another colorless component. It was pressed in a rectangular mold, with loads varying from 15 to 20 kN, into 50 × 25 × 5 mm briquettes, which were subsequently placed into the cell.

A. V. Luikov Heat and Mass Transfer Institute of the Academy of Sciences of Belarus, Minsk. Institute of Structural Macrokinetics, Russian Academy of Sciences, Chernogolovka. Translated from Inzhenerno-Fizicheskii Zhurnal, Vol. 63, No. 2, pp. 140-146, August, 1992. Original article submitted October 17, 1991.

1062-0125/92/6302-0757$12.50

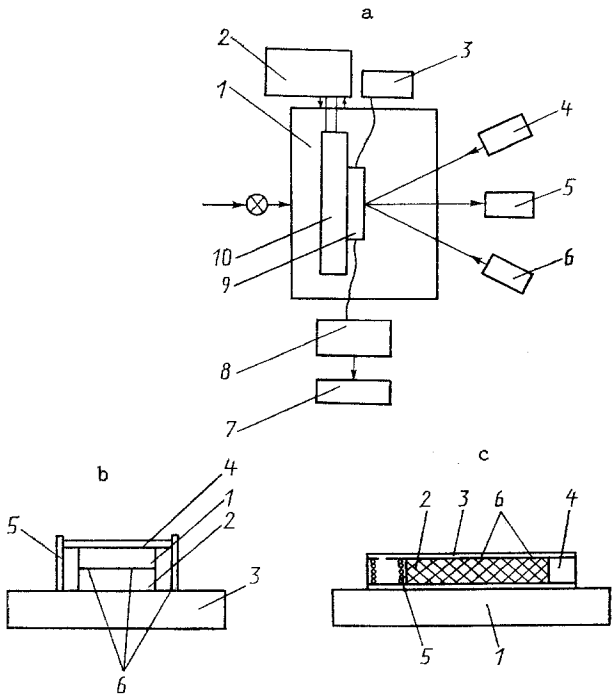

Fig. 1. Experimental setup: a) block diagram [1) constant-temperature shell; 2) thermostat; 3) ignition device; 4, 6) illuminators; 5) video recorder; 7, 8) temperature control; 9) cell; 10) heater]; b) cell for studying the interaction of two crystals [1) malonic acid crystal; 2) piperazine crystal; 3) heater; 4) cover glass; 5) cel; 6) thermocouples]; c) cell for studying the structure of combustion front [1) heater; 2) charge; 3) cover glass; 4) cell; 5) ignition wire; 6) thermocouples].

Methyl orange reddens in an acid medium. After being ground, methyl orange was added to piperazine in proportions of 1% by mass and thoroughly stirred for 3 min in an agate mortar. At this point, the powder became even-yellow in color. Then a stoichiometric quantity of malonic acid was added, and the mixture was pressed into 50 × 25 × 5 mm briquettes.

2. Particle Interaction. For investigating the interaction between two particles, a flat piperazine crystal was selected and laid on the heater, and on top a malonic acid crystal was located using a plane surface and pressed with a cover glass in order to provide a satisfactory thermal contact between the piperazine and malonic acid surfaces. The heater was energized, and after the temperature reached T = 110°C, a visible reaction between the substances was initiated. The briquette for visualizing the processes occurring in the front was placed into the cell, and afterwards the thermostating liquid was thrown in the feed. With the attainment of the required temperature controlled via the thermocouples, the reaction was initiated by ignition.

A protective shell and temperature variation of the medium underneath allow of experiments to be performed in various heat loss conditions. This permits a real-time registration of structural transformations both in the front of the self-propagating synthesis and in individual crystals.

Thermal Analysis Techniques. Thermochemical properties of the chosen system were studied in the Unipan 605 scanning calorimeter. Experimental conditions are set forth in detail in the first part of the article.

Phase transitions were studied using the UIP-70 device, manufactured by the Central Design Office of the Unique Instrument Engineering of the USSR Academy of Sciences. Loads on a measuring rod varied from 0 up to 150 N. A cell was specially fabricated of the material with a small thermal expansion coefficient in the temperature range 20-200°C. A "pellet" 6 mm in diameter, precompressed at a load of 200 N, was placed into the cell. Experimental conditions were maintained similar to those for investigations in the calorimeter. The heating rate was 5 K/min in the range 25-150°C. A gap between the cell and the pump ensured a free stroke of the pump in conformity with variations in the sample height. Prior to the experiment, desiccated high-purity argon was pumped through the heating chamber.

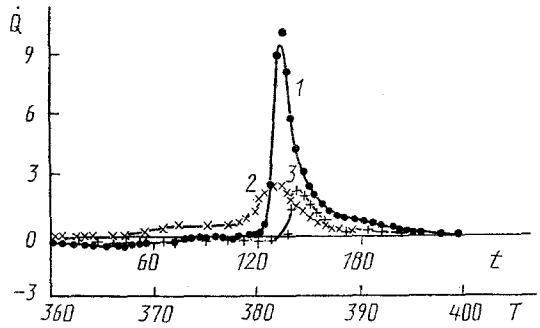

Fig. 2. Effect of molar ratio on heat release with a scanning rate of 10 K/min: 1) stoichiometric ratio; 2) 2 mole piperazine to 1 mole malonic acid; 3) 1 mole piperazine to 2 mole malonic acid. Q̇, kJ/(kg·sec); t, sec; T, K.

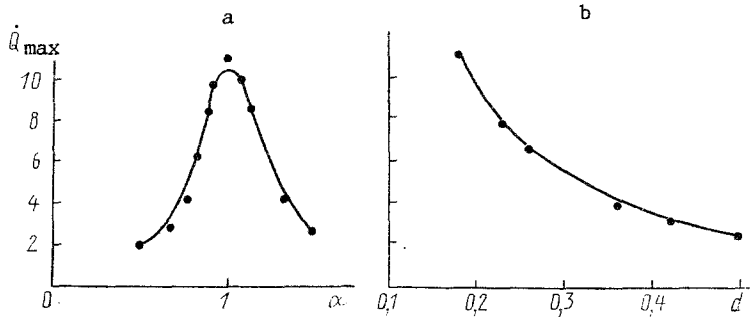

Fig. 3. Effects of molar ratio (a) and particle diameter of the original charge (b) on the maximum of heat release rate. d, mm; $\dot{Q}_{max}$, kJ/(kg·sec).

Discussion of the Results. 1. Thermochemical Studies. Let us determine the quantity of heat released during the chemical reaction in the given system. The experiments conducted with the calorimeter revealed that the melting enthalpies of malonic acid and piperazine are $H^{MA} \sim 197$ kJ/kg and $H^{PP} \sim 251$ kJ/kg. The enthalpy of the product crystallization is $H^{PR} \sim 248$ kJ/kg. The thermal effect recorded during the interaction is $Q_0 \sim 250$ kJ/kg. In accordance with the synthesis stages identified in part 1, during the chemical reaction the following amount of heat is liberated

$$H_{x.p} = Q_0 + H^{MK} + H^{PP} - H^{PR} \cong 450 \text{ kJ/kg}$$

Hence, the chemical reaction proceeds

$$C_4H_{10}N_2 + C_3H_4O_4 \rightarrow C_7H_{14}N_2O_4 + 86 \text{ kJ/mole}$$

The prevalence of piperazine not only noticeably alters the thermal effect and the heat release rate, but also shifts the peak toward the region of lower temperatures (Fig. 2), viz., towards T = 110°C, which is the melting point of piperazine. If malonic acid predominates, a shift toward higher temperatures occurs, viz., toward T = 136°C, which is the melting point of malonic acid. Therefore, only a local melting of malonic acid takes place during synthesis in the calorimeter at a scanning rate of 10 K/min and dispersity of 0.2 ± 0.05 mm.

The maximum of the heat release rate (Fig. 3a) is the greatest when the component ratio is stoichiometric. It reduces abruptly with a deviation from stoichiometry. When the particle diameter (Fig. 3b) of the original charge increases, the maximum of the heat release rate decreases by a parabolic law.

The tests demonstrated that the process proceeds with a variation in the phase state and with subsequent crystallization. Therefore, the dynamics of a change in the sample height was measured. Figure 4 shows the volume modulus as a function of temperature at a scanning rate of 5 K/min. A regression analysis was carried out for this relation and for the kinetic function of heat release:

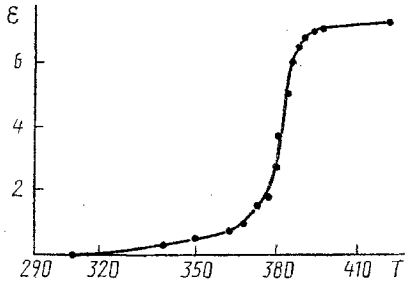

Fig. 4. Decrease in sample height at a scanning rate of 5 K/min. ε, %.

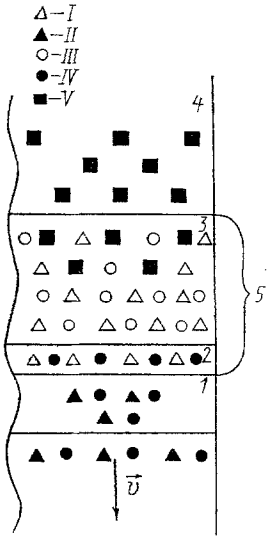

Fig. 5. Structure of the combustion wave: piperazine in liquid (I) and solid (II) phases, respectively; malonic acid in liquid (III) and solid (IV) phases; solid phase of the product (V); and 5 is the synthesis front.

$$\alpha(T) = \int_0^T \dot{Q}(t)\,dt \Big/ \int_0^\infty \dot{Q}(t)\,dt.$$

For temperatures when $\alpha > 50\%$ and there is a 94% correlation between α and ε, it is possible to construct the linear regression with a standard error of 5.4. This implies that, during crystallization, there are sizable pores between the salt crystals, because of which ε varies.

2. Structural Transformations in the Synthesis Front. To visualize the processes we used the tracer methyl orange at a pH of 3.0-4.4. With its aid we managed to record the effect of initial temperature, the dynamics of structural transformations, the front stopping, and the initial acceleration section.

Another independent method of visualizing the structural transformations consisted in adding one of the components of base or acid fluorescein to the powder. This enabled us to observe the front movement and the luminescence of its individual zones. The zones of relevant melts with luminophor proved to fluoresce fairly intensely, unlike the reaction product and the original components. A fluorescence zone of the piperazine melt is distinguished by a bright green color. A greenish wide region corresponds to the acid zone fluorescence.

A zone of the base melt, with the acid still solid, is narrower by 5-6 fold than a zone in which the acid melt also exists.

To ensure the autowave mode for the selected dimensions of the sample (for a height of 5 mm), $T_0 > 70°C$ was kept. A buildup of the compacting pressure reduced the jaggedness of the front and brought it closer to flat. At a compacting pressure $p = 700$ N/cm^2, the velocity of the front appeared maximal ($T_0 = 75°C$).

A wide front (of size 3-4 mm) corresponds to a pressure $p = 500$ N/cm^2 at $T_0 = 75°C$, whereas at $T_0 > 80°C$ it is narrower by an order of magnitude (0.3-0.4 mm). By varying T, we, in fact, regulate heat removal from the combustion zone, which allows us to obtain either a wide or a narrow combustion front. In the case of a wide front, the product crystals are about 2 mm in size, while for a narrow front they are smaller than 0.5 mm. The pore size is, accordingly, equal to about 1 and 0.2 mm. At the instant of the reaction initiation, the front is arched because of an inevitable nonuniformity of the heater characteristics. Further, on the initial acceleration section (of 5-7 mm), the front levels off and becomes flat.

3. Front Stopping. The experiment was performed at the room temperature $T_0 = 20°C$ and a compacting pressure $p = 200$ N/cm^2 in a cylindrical sectional reactor. It was located in a massive copper pig in order that the initial acceleration section should end over the pig surface (>1.5 cm). The mixture ignition was effected from above. After the experiment cessation the reactor was dismounted. A pronounced red zone of the front with the acid melt is visible. Rather than being continuous, the zone has the appearance of separate aggregations. In addition, the original charge and the reaction product are of different coloring. In these experiments, it is clearly seen that the envelope, shielding from heat losses, forms out of the charge even ahead of the zone, where heat removal to the copper pig begins. The width of the shielding envelope constitutes in the experiments was 3 mm, which is consistent with temperature profiles in the wave. During combustion one can see how this envelope and the local reddish regions of sizes comparable to those of the original mixture particles emerge. A leading edge of the envelope, following the synthesis front, is strongly jagged and moves randomly. The velocity of the front, measured visually, was 0.4 mm/sec. In the experiments where the base fluorescein was added to piperazine, a flat front was observable, which represented a thin fluorescent strip of about 0.2 mm in size followed by a dark zone of about 0.5 mm in size, i.e., fluorescence is extinguished as the front becomes "acid."

It is appropriate to point out that the product formation is accompanied by crystallization. In this case, self-purification characteristic of crystallization arises, i.e., the dyes are withdrawn to the pores as isolated inserts [3].

4. Crystal Interaction. A piperazine plate was located in the cell (see Fig. 1b), and a fluorescein-dyed malonic acid was placed on top of the plate. On attaining $T = 110°C$ by the substrate, a visible reaction was initiated. Piperazine melts and gets absorbed by the adjoining face of the malonic acid crystal, forming a product different in color. At this point, the malonic acid crystal breaks down and melts at the faces. As the process evolves, fresh portions of the melt get absorbed by the malonic acid crystal, and the product layer grows.

5. Dynamics of Structural Transformations. Figure 5 schematically represents the synthesis structure based on the results of the process visualization: 1 is the heating zone; 2 is the zone of molten piperazine; 3 is the zone of malonic acid melt, where the major heat release occurs; and 4 is the cooling zone.

Depending on the heat removal rate, three modes of the self-propagating synthesis can be discriminated. With the first mode, heat exchange is insignificant; the front is narrow and flat, and the movement velocity is maximal.

With increasing heat removal rate, the front widens by an order of magnitude and becomes jagged, the velocity fluctuation grows, and the wave velocity falls. The spread in the grain sizes of the product becomes appreciably greater.

At a high-rate heat removal a shielding envelope originates. Only the leading edge of the front is visible, i.e., the front becomes infinitely wide. The envelope width is defined by the relations given in [4]. With a thickness of the charge layer greater than a critical value, the so-called adiabatic combustion with a wide front proceeds. If the thickness is critical, extinction occurs. Thus, visualizing the structural transformations allows not only an identification of the structural pattern of the front, but also an ascertainment of qualitative features of the processes proceeding on the initial acceleration section upon the front stopping. It follows from the above-given results that an autowave process can occur in the given system only with a melting of malonic acid.

6. Estimates of the Wave Parameters. The activation energy of the process studied was taken from [5], viz., $E = 94$ kJ/mole. The adiabatic combustion temperature is:

$$T_a = T_0 + Q/C_p = 157° \text{ C}.$$

Let us evaluate the thermal parameters in the synthesis wave:

$$\beta = R(C_pT_0 + Q)/C_pE = 3{,}8 \cdot 10^{-2} \text{ and}$$

$$\gamma = R(C_pT_0 + Q)^2/C_pEQ = 1{,}2 \cdot 10^{-1}.$$

For these values, the following inequality is fulfilled:

$$9{,}1\gamma - 2{,}5\beta > 1,$$

which is required in [6] for implementing a steady combustion mode. We estimate the width of the shielding envelope from the relationship [7]:

$$\delta = ea_f/V_a\,[(E\,(T_a - T_0)/RT_0^2)^{1/2} - (\lambda_f\rho_f C_f/\lambda_i\rho_i C_i)^{1/2}S/L],$$

where $S = (a_f a_i)^{1/2}/V$ is the heating depth of the inert material; L is its width; a, λ, ρ, and C are, correspondingly, the thermal diffusivity, thermal conductivity, density, and specific heat (the subscripts are as follows: f refers to the charge and i denotes the material of which the reactor is fabricated); T_a is the adiabatic temperature, and V is the wave velocity.

For the case considered δ = 2.7 mm, which is in agreement with experimental data.

Thus, the approach presented permits an examination of structural, phase, and chemical transformations occurring in the synthesis wave.

The authors are grateful to I. M. Gulis for fruitful discussion and remarks.

LITERATURE CITED

1. A. G. Merzhanov and É. N. Rumanov, Usp. Fiz. Nauk, **151**, No. 4, 553-593 (1987).
2. B. P. Nikolskii (ed.), Handbook for a Chemist, Vol. 2 [in Russian], Moscow (1969).
3. A. A. Chernov, E. I. Givargizov, Kh. S. Bagdasarov, et al., Modern Crystallography. Crystal Formation, Vol. 3 [in Russian], Moscow (1980).
4. S. S. Rybanin and S. L. Sobolev, Fiz. Goreniya Vzryva, **25**, No. 5, 16-25 (1989).
5. E. G. Klimchuk, G. M. Avetisyan and A. G. Merzhanov, Dokl. Akad. Nauk SSSR, **311**, No. 5, 1161-1164 (1990).
6. A. G. Merzhanov, in: Physical Chemistry. Modern Problems [in Russian], Ya. M. Kolotyrkin (ed.), Moscow (1983), pp. 6-44.
7. M. A. Konstantinova-Shlezinger (ed.), Luminiscent Analysis [in Russian], Moscow (1961).